

A simple fully conformal solution of Einstein's gravitational equations and the agreement of its implications with astrophysical data

Richard Dvorsky richard.dvorsky@vsb.cz

¹Nanotechnology Centre, ²Centre for Advanced Innovation Technologies, ³Faculty of Materials Science and Technology, VSB – Technical University of Ostrava, 17. listopadu 15/2172, Ostrava, 708 00, Czech Republic

key words: distances and redshifts, gravitation, gamma-ray burst, quasars, cosmological parameters, gravitation

ABSTRACT

Another cosmological redshift mechanism could exist in general relativity, as is differences in the global metric field $g_{\mu\nu}$ between the radiation source in the past, and the observer in the present, known as gravitational redshift in massive stars. In this paper, we present a fully conformal global metric model with time scaling that would lead to the above alternative interpretation of the cosmological redshift. It is based on a relatively simple global solution of Einstein's gravitational equations without the cosmological term, and the analysis also shows other interesting astrophysical implications. The model naturally solves the problem of critical density and spatial flatness, as well as the problem of cosmological redshift in the spectra of distant astrophysical sources, and the problem of Olbers' and Seeliger's paradox. At the same time, it replaces the strict causal horizon principle with a much softer formulation - the region of the practically observable universe. Confrontation with astrophysical data provides interesting agreement with the spatial distribution of astrophysical radiation sources such as γ -ray bursts and quasars. However, probably the most important consequence is the new, generalized formulation of Hubble's law $z(r) = (e^{Hr/c} - 1)$, which shows good agreement $R^2 \approx 0.9824$ with experimental data even for very distant sources. The paper also physically justifies in principle the modification of Newton's law of gravity for infinite space proposed by Seeliger. The modifying exponential term $e^{-Hr/c}$ is uniquely quantified by the Hubble parameter and the speed of light.

1. INTRODUCTION

At present, the widely accepted explanation for the cosmological redshift is a spatial expansion with a time origin in the Big Bang, assumed within the standard cosmological model. The motivation for writing this paper was the question of whether the But could the cosmological redshift be alternatively interpreted as the difference between the global metric field around a radiative astrophysical source in the past and the global metric field around the observer in the present? This interpretation should correspond to a global solution of Einstein's gravitational equations whose metric field varies in time, while respecting the required conservation of the laws of nature. One solution that satisfies the above requirements is a fully conformal global metric with a time scaling, which is derived in this paper and then discussed in confrontation with astrophysical data. A number of mainly theoretical papers have been published in the area of conformal solution of Einstein's gravity equations [1], [2], [3], [4], [5], [6], [7], including conformal forms of the well-known Robertson-Walker metric [8]. The fully conformal global metric with a time scaling is derived based on three simplifying approximations: "Extrapolation of Einstein's gravitational equations to a global cosmological scale is the correct description of the geometry of the physical universe", "The spatial distribution of energy is homogeneous and isotropic on the global cosmological scale, and does not depend on time", and "the local reference observer system has a Minkowski metric". In contrast to the strongly theoretical character of the above papers, our derived global metric is confronted with astrophysical data such as cosmological redshift and the observable spatial distributions of quasars and γ -ray bursts and at the same time successfully explains Olbers' paradox and Seeliger's gravitational paradox for infinite spacetime.

2. FULLY CONFORMAL SPACETIME WITH TIME SCALING

Let the coordinates' origin of the local inertial system (observer location), in which the microwave background of the universe is isotropic, be our "central observer point" (in next text COP). It can be located at any place and time (*for simplicity let us accept the condition of local absence of gravitational bodies*). Taking into account the experimentally confirmed spatial flatness in the vicinity of the COP, we establish Minkowski coordinates $\mathbf{x}^o = (x^o_1, x^o_2, x^o_3, x^o_4 = ct^o)$ for this local inertial system with the origin just at the COP. Since the real universe allows an infinite number of alternative COP, we restrict ourselves to a single one for the following analysis, with the above coordinate system \mathbf{x}^o , which parameterizes the global metric field of the universe $g(\mathbf{x}^o)$. All further considerations are based on the following assumptions:

APROXIMATION 1: Extrapolation of Einstein's gravitational equations [9] to a global cosmological scale is the Correct description of the geometry of the physical universe.

APROXIMATION 2: The spatial distribution of energy is homogeneous and isotropic on the global cosmological scale, and does not depend on time.

APROXIMATION 3: The local reference observer system has a Minkowski metric. $\lim_{x_4^o \rightarrow 0} g_{\mu\nu}(x_4^o) = \eta_{\mu\nu}$

Let us find solutions of Einstein's gravity equations without a cosmological constant in the form of a fully conformal Minkowski metric $\eta_{\mu\nu}$ with purely temporal global scaling $\psi(x_4^o)$

$$R_{\mu\nu} - \frac{1}{2}Rg_{\mu\nu} = \kappa T_{\mu\nu} \quad \dots \quad \left\{ \begin{array}{l} g_{\mu\nu}(x_4) = \psi(x_4)\eta_{\mu\nu} = \psi(x_4) \begin{pmatrix} 1 & 0 & 0 & 0 \\ 0 & 1 & 0 & 0 \\ 0 & 0 & 1 & 0 \\ 0 & 0 & 0 & -1 \end{pmatrix} \\ ds^2 = g_{\mu\nu}(x_4)dx_\mu dx_\nu = \psi(x_4)(dx_1^2 + dx_2^2 + dx_3^2 - dx_4^2) \end{array} \right. \quad (1)$$

From the corresponding Christoffel symbols $\Gamma^{\mu}_{\nu\lambda}$ as functions of single time variable x_4 , only the following functions are nonzero for the conformal metric tensor (1) [APPENDIX 1](#):

$$\Gamma^{\mu}_{\nu\lambda}(x_4) = \frac{1}{2}g^{\mu\alpha}(x_4)(\partial_\nu g_{\alpha\lambda}(x_4) + \partial_\lambda g_{\alpha\nu}(x_4) - \partial_\alpha g_{\nu\lambda}(x_4)) \quad . \quad (2)$$

$$\left. \begin{array}{l} \Gamma^1_{14}(x_4) = \Gamma^1_{41}(x_4) \\ \Gamma^2_{24}(x_4) = \Gamma^2_{42}(x_4) \\ \Gamma^3_{34}(x_4) = \Gamma^3_{43}(x_4) \\ \Gamma^4_{11}(x_4) = \Gamma^4_{22}(x_4) = \Gamma^4_{33}(x_4) = \Gamma^4_{44}(x_4) \end{array} \right\} = \frac{1}{2}\partial_4 \ln \psi(x_4)$$

The following Ricci tensor is non-zero only in the diagonal components, and the scalar curvature R is also a non-zero function of single time variable x_4 [APPENDIX 3](#).

$$\begin{aligned} R_{11} = R_{22} = R_{33} &= \frac{1}{2}\partial_4^2 \ln \psi(x_4) + \frac{1}{2}(\partial_4 \ln \psi(x_4))^2 \\ R_{44} &= -\frac{3}{2}\partial_4^2 \ln \psi(x_4) \\ R &= \left(-3\partial_4^2 \ln \psi(x_4) - \frac{3}{2}(\partial_4 \ln \psi(x_4))^2 \right) \psi^{-1}(x_4) \end{aligned} \quad . \quad (3)$$

While the purely spatial part of the 3D has the character of a flat space E3 [10], the total global curvature R of the spacetime according to (1) is generally non-zero. In a uniform (homogeneous and isotropic) universe, the energy-momentum tensor $T_{\mu\nu}$ on a global cosmological scale can be approximated by a model of an ideal static fluid with energy density ε and pressure p , independent on time

$$T_{\mu\nu} = \begin{pmatrix} p & 0 & 0 & 0 \\ 0 & p & 0 & 0 \\ 0 & 0 & p & 0 \\ 0 & 0 & 0 & \varepsilon \end{pmatrix}, \quad \partial_4 T_{\mu\nu} = 0. \quad (4)$$

After substituting the energy-momentum tensor (4) into (1), we obtain conditions for a currently unknown scaling function $\psi(x_4)$ [APPENDIX 4](#).

$$R_{\mu\nu} - \frac{1}{2}Rg_{\mu\nu} = \kappa T_{\mu\nu} \rightarrow \left\{ \begin{array}{l} R_{11} - \frac{1}{2}R\psi(x_4)\eta_{11} = \kappa p \\ R_{22} - \frac{1}{2}R\psi(x_4)\eta_{22} = \kappa p \\ R_{33} - \frac{1}{2}R\psi(x_4)\eta_{33} = \kappa p \\ R_{44} - \frac{1}{2}R\psi(x_4)\eta_{44} = \kappa\varepsilon \end{array} \right. \rightarrow \begin{array}{l} -\partial_4^2 \ln \psi(x_4) - \frac{1}{4}(\partial_4 \ln \psi(x_4))^2 = \kappa p \\ \frac{3}{4}(\partial_4 \ln \psi(x_4))^2 = \kappa\varepsilon \end{array} \quad . \quad (5)$$

The solution of equation (5)-(b) gives a general form of the scaling function $\psi(x_4)$

$$\psi_{\pm}(x_4) = \psi(0)e^{\pm x_4 \sqrt{\frac{4}{3}\kappa\varepsilon}}. \quad (6)$$

The problem of alternatives $\psi_-(x_4)$ and $\psi_+(x_4)$ of the scaling function (6) will be discussed below.

APPROXIMATION 3: The local reference observer system has a Minkowski metric. $\lim_{x_4^o \rightarrow 0} g_{\mu\nu}(x_4^o) = \eta_{\mu\nu}$

With respect to APPROXIMATION 3, the scaling function (6) becomes:

$$\psi_{\pm}(x_4) = e^{\pm x_4 \sqrt{\frac{4}{3}\kappa\varepsilon}}. \quad (7)$$

The 3D space has a Euclidean metric E3 with zero scalar curvature at each time frame [APPENDIX 2](#) and [APPENDIX 5](#). However, the scalar curvature R of spacetime is non-zero and with respect to (1), (3) and (6), it is described by (see [APPENDIX 6](#))

$$R(\psi_{\pm}(x_4)) = 2\kappa\varepsilon e^{\mp x_4 \sqrt{\frac{4}{3}\kappa\varepsilon}} \geq 0, \quad (8)$$

and is in all cases a function of the time coordinate x_4 . In the vicinity of the local observer $x_4 \rightarrow 0$, the total spacetime curvature takes on an extremely low positive value of the order of 10^{-35} s^{-2} , which cannot be distinguished from Minkowski spacetime by existing methods. Minkowski geometry of the local spacetime in the vicinity of $x_4 \rightarrow 0$ is thus consistent with experimental experience.

The conformal solution $g_{\mu\nu}(x_4)$ of Einstein's gravitational equation (1) with the scaling function (7) gives explicit conditions for the corresponding equation of state. According to the nature of the scaling function (7) we can write $\partial_4^2 \ln \psi(x_4) = 0$, and the solution of the equation system (5) (a) and (b) is the final equation of state of corresponding conformal spacetime

$$\left. \begin{aligned} -\frac{1}{4}(\partial_4 \ln \psi(x_4))^2 &= \kappa p \\ \frac{3}{4}(\partial_4 \ln \psi(x_4))^2 &= \kappa\varepsilon \end{aligned} \right\} \rightarrow \boxed{3p + \varepsilon = 0}. \quad (9)$$

3. COSMOLOGICAL REDSHIFT

Let us analyse the relative time flow at different radial distances from the COP. The spacetime interval $ds(\mathbf{x})$ is a function of the four-vector $\mathbf{x}(x_1, x_2, x_3, x_4)$ due to the generally varying metric tensor $\mathbf{g}_{\mu\nu}(\mathbf{x})$. Similarly, the Minkowski coordinates $(x^o_1(\mathbf{x}), x^o_2(\mathbf{x}), x^o_3(\mathbf{x}), x^o_4(\mathbf{x}))$ of the local inertial systems around any point \mathbf{x} of spacetime, are a function of the four-vector \mathbf{x}

$$ds(\mathbf{x})^2 = \frac{g_{11}(\mathbf{x})dx_1^2}{\eta_{11}dx_1^o(\mathbf{x})^2} + \frac{g_{22}(\mathbf{x})dx_2^2}{\eta_{22}dx_2^o(\mathbf{x})^2} + \frac{g_{33}(\mathbf{x})dx_3^2}{\eta_{33}dx_3^o(\mathbf{x})^2} + \frac{g_{44}(\mathbf{x})dx_4^2}{\eta_{44}dx_4^o(\mathbf{x})^2}. \quad (10)$$

If the chosen position of the COP in spacetime is denoted by $\mathbf{x}(0, 0, 0, 0) \equiv \mathbf{0}$, then the Minkowski $(x^o_1(\mathbf{0}), x^o_2(\mathbf{0}), x^o_3(\mathbf{0}), x^o_4(\mathbf{0}))$ of the corresponding local inertial frame in the conformal metric (1) according to (7) coincide with the geodetic coordinates (x_1, x_2, x_3, x_4) in the vicinity of $\mathbf{0}$ (which is consistent with the Minkowski metric of the surrounding spacetime, confirmed by experimental experience - 3D-spatial flatness and a large region with negligible redshift)

$$ds(\mathbf{0})^2 = \frac{[g_{11}(\mathbf{0}) = \eta_{11}]dx_1^2}{\eta_{11}dx_1^o(\mathbf{0})^2} + \frac{[g_{22}(\mathbf{0}) = \eta_{22}]dx_2^2}{\eta_{22}dx_2^o(\mathbf{0})^2} + \frac{[g_{33}(\mathbf{0}) = \eta_{33}]dx_3^2}{\eta_{33}dx_3^o(\mathbf{0})^2} + \frac{[g_{44}(\mathbf{0}) = \eta_{44}]dx_4^2}{\eta_{44}dx_4^o(\mathbf{0})^2}. \quad (11)$$

There is a well-known formula for the own time flow τ in a point event ($dx_i = 0, i = 1, 2, 3$) at the COP $\mathbf{0}$ at any point \mathbf{x} in spacetime [\[11\]](#), [\[12\]](#)

$$\left. \begin{aligned} \eta_{44}dx_4^o(\mathbf{x})^2 &= g_{44}(\mathbf{x})dx_4^2 \\ \eta_{44}dx_4^o(\mathbf{0})^2 &= g_{44}(\mathbf{0})dx_4^2 \end{aligned} \right\} \rightarrow dx_4^o(\mathbf{x}) = dx_4^o(\mathbf{0})\sqrt{\frac{g_{44}(\mathbf{x})}{g_{44}(\mathbf{0})}} \rightarrow d\tau(\mathbf{x}) = d\tau(\mathbf{0})\sqrt{\frac{g_{44}(\mathbf{x})}{g_{44}(\mathbf{0})}}. \quad (12)$$

Within the conformal metric (1), the (12) takes the form of

$$d\tau(x_4) = d\tau(0)\sqrt{\psi(x_4)}. \quad (13)$$

As a result of the assumption of the conformal metric (1) and relation (7), the equation (13) takes the form

$$d\tau(x_4) = d\tau(0)\sqrt{\psi_{\pm}(x_4)} = d\tau(0)e^{\pm x_4\sqrt{\frac{\kappa\epsilon}{3}}}. \quad (14)$$

The negative time coordinate x_4 of the past defines a radial "observation sphere" with radius r with respect to the COP

$$\left. \begin{aligned} dr^2 &= dx_1^2 + dx_2^2 + dx_3^2 \\ ds(x_4)^2 &= 0 \end{aligned} \right\} \rightarrow \psi(x_4)dr^2 - \psi(x_4)dx_4^2 = 0 \rightarrow dr = -dx_4 \rightarrow r = -x_4. \quad (15)$$

If two different points emit light from a source with the same frequency $\nu(0)$, then we measure an identical value of $\nu(0)$ for a source at $r = 0$ near the COP, while for a source at a large distance r the frequency will theoretically be higher or lower depending on the polarity of the exponent in (14)

$$\nu(r) = \nu(0)e^{\mp r\sqrt{\frac{\kappa\epsilon}{3}}}. \quad (16)$$

At this stage, the polarity of the exponent (16) can be decided based on experimental experience. Since a positive sign would represent a blue cosmological shift, it is appropriate to see it as "non-physical" for now, but this does not exclude its possible meaning in the future. On the contrary, a red cosmological shift ($\nu(r) < \nu(0)$) has been clearly confirmed experimentally, and therefore we will accept only the negative sign.

$$\nu(r) = \nu(0)e^{-r\sqrt{\frac{\kappa\epsilon}{3}}}, \quad (17)$$

Let's reformulate the (16) to the "redshift" equation

$$z \stackrel{\text{def}}{=} \frac{\nu(0) - \nu(r)}{\nu(r)} \rightarrow z = e^{r\sqrt{\frac{\kappa\epsilon}{3}}} - 1, \quad (18)$$

which converges into the familiar linear form for small values of the exponent (small distances r from the COP)

$$z = \left(e^{r\sqrt{\frac{\kappa\epsilon}{3}}} \approx r\sqrt{\frac{\kappa\epsilon}{3}} + 1 \right) - 1 \rightarrow z = \left[\sqrt{\frac{\kappa\epsilon}{3}} \right] r. \quad (19)$$

Equation (19) is formally equivalent to a linear formulation of the standard Hubble's law for small cosmological distances

$$z = \frac{H}{c} r. \quad (20)$$

Combining (19) and (20), we get a final form that allows us to directly calculate the average mass density of the universe ρ using experimental parameters. Its value corresponds to the critical density ρ_{crit} [13] for the flat space solution of the Friedmann model

$$\left. \begin{aligned} \frac{H}{c} &= \sqrt{\frac{\kappa\epsilon}{3}} \\ \kappa &= \frac{8\pi G}{c^4} \end{aligned} \right\} \rightarrow \left\{ \rho = \frac{3H^2}{8\pi G} = \rho_{\text{crit}} = 8 \cdot 10^{-27} \text{ kgm}^{-3} \right\} \rightarrow \boxed{\nu(r) = \nu(0)e^{-\frac{H}{c}r}}. \quad (21)$$

Based on this match, the equation (18) can be expressed as the final form of the generalized Hubble's law

$$\boxed{z = e^{\frac{H}{c}r} - 1}. \quad (22)$$

Its nonlinear character is clearly visible only at large cosmological distances r (see [Obr. 1](#))

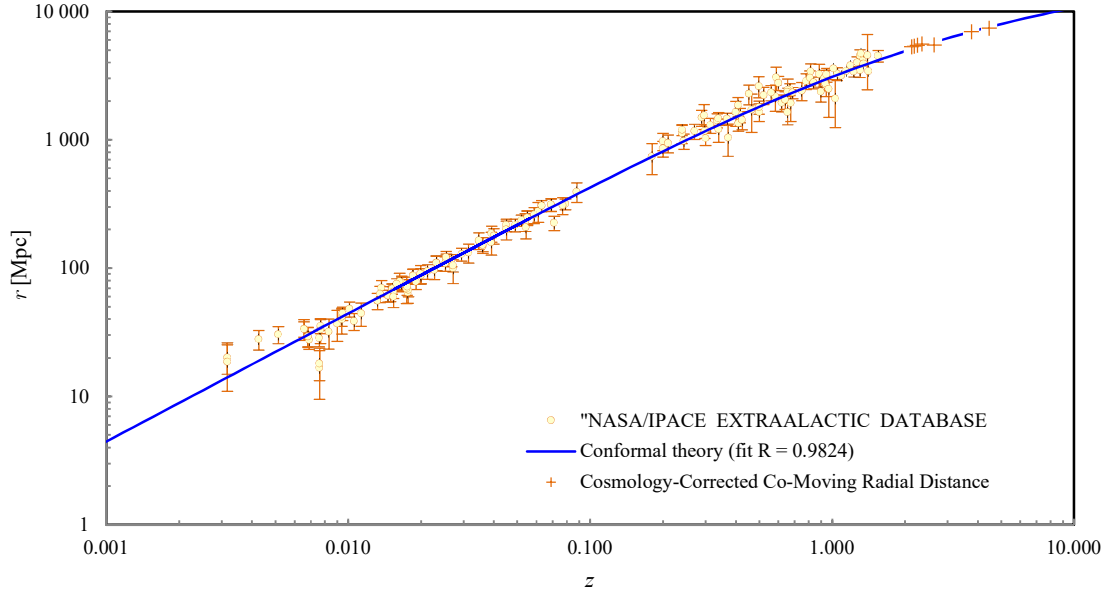


Fig.1 Hubble diagram - experimental points are taken from NASA/IPACE EXTRAGALACTIC DATABASE [14] and the blue curve — represents the fit of the generalized Hubble's law (22) for the Hubble's parameter 69.7 [kms⁻¹/Mpc] [15].

The coefficient of determination $R^2 = 0.9824$ of the fit in Fig. 1 documents a good agreement with the experimental data and confirms the realistic nature of the mathematical formula of the generalized Hubble's law (22). In this situation, it is worth pointing out that its nonlinearity is a direct consequence of the conformal solution of Einstein's gravitational equations (1) without the cosmological term and it does not require the hypothetical concept of dark energy, which is necessary to solve this problem within the standard Λ CMD model. Based on relations (19) and (20), the scaling function (7) and hence the metric tensor $g_{\mu\nu}$ takes a particular form

$$\left. \begin{array}{l} \psi(x_4) = e^{x_4 \sqrt{\frac{4}{3}\kappa\varepsilon}} \\ x_4 = -r \end{array} \right\} \rightarrow \left\{ \begin{array}{l} \psi(r) = e^{-\frac{2H}{c}r} \rightarrow g_{\mu\nu}(x_4) = e^{-\frac{2H}{c}r} \eta_{\mu\nu} \\ ds(r)^2 = \underbrace{e^{-\frac{2H}{c}r}}_{dx_1^{\circ 2}} dx_1^2 + \underbrace{e^{-\frac{2H}{c}r}}_{dx_2^{\circ 2}} dx_2^2 + \underbrace{e^{-\frac{2H}{c}r}}_{dx_3^{\circ 2}} dx_3^2 - \underbrace{e^{-\frac{2H}{c}r}}_{dx_4^{\circ 2}} dx_4^2 \end{array} \right. \quad (23)$$

This metric must be understood as an universal effect to which all other interactions are absolutely subjugated, and the metric field has a completely different character in this sense. It is not an interacting agent like other fields, but it is the carrier of the very laws of dynamics by its geometrical nature.

4. SPATIAL DISTRIBUTION OF γ -RAY BURSTS

Another cosmological test of the conformal Minkowski metric hypothesis can be an experimental verification of the natural homogeneous distribution of matter on a global cosmological scale. Such a test can be performed by observing highly specific astrophysical objects and events such as black holes, quasars, and ultimately γ -ray sources that can be understood as standards (the distribution of galaxies is inappropriate for such a test due to their highly non-standard diversity). We will discuss the spatial distribution of γ -ray bursts in the following chapter. In [16] they published a methodology for applying the V/V_{\max} test to γ -ray sources and subsequently performed a constrained analysis of the spatial distribution for 140 sources [17]. The result shows an increasing deficit in the observed number of low intensity sources. Assuming an identical nature of the sources and the standard Euclidean flat-space metric E3, these results can be interpreted as a decrease in source density towards the past within a fully conformal spacetime. Such an interpretation leads to the conclusion that the γ -ray density changes over time on a global scale.

Let us now perform a similar analysis under a hypothetical conformal metric. The time-independent nature of the energy-momentum tensor (9) requires a global density of γ -ray sources invariant over time. The number of sources N within in a sphere of radius r_{\max} around the COP is given by the time-invariant global source density $n_{\gamma 0}$:

$$N(r_{\max}) = n_{\gamma o} \frac{4}{3} \pi r_{\max}^3. \quad (24)$$

In the mentioned V/V_{\max} test [16], the ratio of the intensity C_{\max} of the farthest source at distance r_{\max} to the threshold intensity C_{\min} at the detection limit is chosen as the independently variable distribution parameter. The intensity of the source C_{\max} decreases not only with the inverse square of the distance r_{\max} but also due to the time-varying metric (23). As a result, the intensity on a model source surface of radius R decreases with distance r_{\max} from the observer

$$\left. \begin{aligned} C_{00}(R) &= \frac{\overset{\text{def}}{d^2 E}}{dS^\circ dt^\circ} \\ C_0(R) &= \frac{\overset{\text{def}}{d^2 E}}{dS dt} \end{aligned} \right\} \rightarrow C_0(R) = \frac{d^2 E}{dS dt} \rightarrow C_0(R) = C_{00}(R) \frac{dS^\circ dt^\circ}{dS dt}. \quad (25)$$

As a consequence of the conformal metric (23) we can write

$$dx_\mu^\circ = e^{-\frac{H}{c} r} dx_\mu \rightarrow \left\{ \begin{aligned} dx_4^\circ &= e^{-\frac{H}{c} r} dx_4 \rightarrow dt^\circ = e^{-\frac{H}{c} r} dt \\ dS &\approx dx_1 dx_2 \\ dS^\circ &\approx dx_1^\circ dx_2^\circ = e^{-\frac{2H}{c} r} dx_1 dx_2 \end{aligned} \right\} \rightarrow \frac{dS^\circ dt^\circ}{dS dt} = e^{-\frac{3H}{c} r}, \quad (26)$$

and for the radiation intensity on a model source surface of radius R it is

$$C_0(R) = C_{00}(R) e^{-\frac{3H}{c} r_{\max}}. \quad (27)$$

As a result of the consequent decrease in intensity with the square of the distance, the following applies:

$$C_{\max} = C_0(r_{\max}) = C_{00}(R) \frac{R^2}{r_{\max}^2} e^{-\frac{3H}{c} r_{\max}}. \quad (28)$$

The NSSTC, BATSE4B astrophysical database [18] contains data as dependence of the number of sources on the ratio of the minimum intensity to the threshold intensity $N(C_{\max}/C_{\min})$. For the purpose verifying hypothesis of the universe with the conformal metric (1), (23), we refine the equation (28) to

$$\frac{C_{\max}}{C_{\min}} = \left(C_{00}(R) \frac{R^2}{C_{\min}} \right) e^{-\frac{3H}{c} r_{\max}} r_{\max}^{-2}. \quad (29)$$

The mutual dependence of the two parameters then comes from the simultaneous validity of (24) and (29):

$$\left\{ \begin{aligned} A &= \left(\frac{C_{00}(R)}{C_{\min}} R^2 \right) \left(\frac{3}{4\pi n_{\gamma o}} \right)^{\frac{2}{3}} [-] \\ B &= 3 \frac{H}{c} \left(\frac{3}{4\pi n_{\gamma o}} \right)^{\frac{1}{3}} [-] \end{aligned} \right\} \rightarrow \boxed{\frac{C_{\max}}{C_{\min}} = AN^{-\frac{2}{3}} e^{-BN^{\frac{1}{3}}}} \quad (30)$$

The fit of the theoretical dependence (30) to the mentioned experimental data of NSSTC, BATSE4B [18] is shown in Fig. 2.

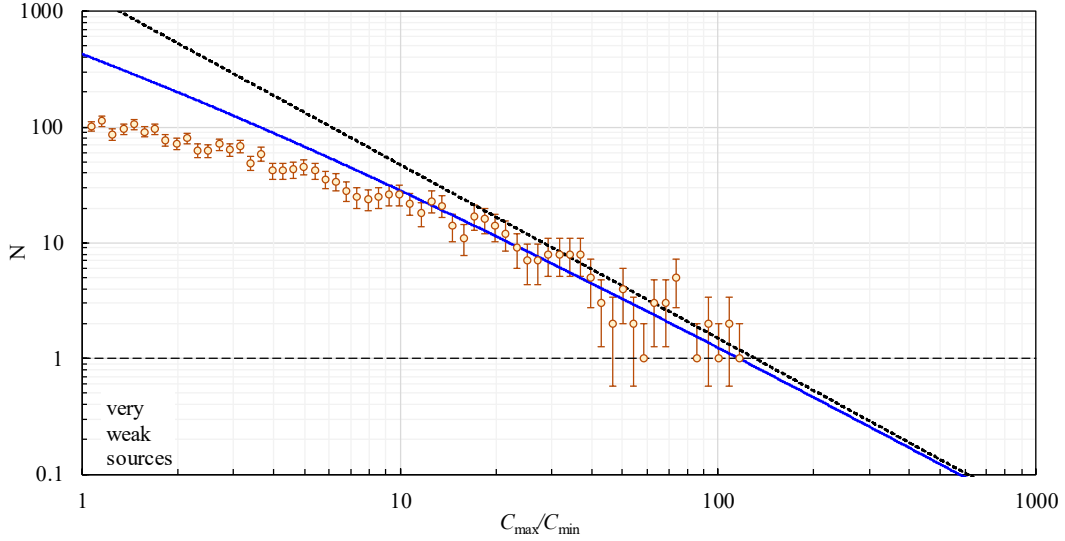


Fig. 2 Theoretical fit — distribution of the total number N of γ -ray burst sources as a function of the C_{\max}/C_{\min} ratio for 2372 measured sources ($A = 130$, $B = 0.12$). The black dashed line would correspond to a uniform distribution of sources in flat space with the standard Euclidean metric E3, as indicated by a formal extrapolation of the plot below the single-source detection level of $N = 1$.

The first requirement of the fit is the limit transition $B \rightarrow 0$ of formula (30) to the standard version of the Minkowski metric for small distances from the COP, which shows asymptotic behaviour for well-detectable sources with large C_{\max} corresponding to smaller r_{\max} . The fit has a coefficient of determination $R^2 \approx 0.888$ in the region $C_{\max}/C_{\min} \geq 10$. The above fit for $B = 0.12$ gives a time-invariant global γ -ray burst density of $n_{\gamma} \approx 1.47 \cdot 10^{-75} \text{ m}^{-3} \approx 43 \text{ Gpc}^{-3}$ according to (30).

The detection of the vast majority of strong sources in the nearby region is highly probable both in terms of their high intensity and their frequency of occurrence in a relatively small volume of the vicinity of the COP. However, in more distant regions, the detection probability is negatively affected both by the decreasing intensity of the sources and by their more difficult localization in an extremely increasing volume. Detection of "missing" sources could therefore serve as one way to verify or falsify this hypothesis of a global conformal metric of the universe.

5. SPATIAL DISTRIBUTION OF QUASARS

D. Sciama and M. Rees published a paper in 1966 [19] with the intention of falsifying the steady state theory of the universe. The paper showed that the frequency of observed quasars depends on the magnitude of the redshift, and from this fact he deduced a time evolution of the source density that contradicts the ideas of the steady-state model of the universe. This raises the question of how to correctly interpret observations of sources with different redshift values. Although the predicted time evolution of the source density was contrary to steady-state concepts, it has not been explained in principle even within the standard Λ CMD cosmological model. It is associated with the general assumption of the genesis and evolution of astrophysical objects within any cosmological theory with a time origin. Of course, the time evolution cannot be excluded even in models without said beginning, because the limited observational experience might elude us from the global mechanisms ("Too brief glimpse into the past from the beginning of summer may lead one to believe that the world was created in winter").

Thus, we examine whether the hypothesis of the conformal metric is consistent with the assumption that the distribution of quasars seems to be homogeneous in space from the COP. For a time-invariant global source density n_{q_0} , the number of sources dN contained in a differential spherical shell of radius r around the COP is given by

$$dN = n_{q_0} 4\pi r^2 dr. \quad (31)$$

Now we derive the distribution of dN/dz as a function of redshift from all observed quasars. From the generalized Hubble's law (22), the radial parameters r and dr on the left-hand side of equation (31) can be expressed as a function of the redshift z

$$z = e^{\frac{H_r}{c}} - 1 \rightarrow \begin{cases} r = \frac{c}{H} \ln(z + 1) \\ \frac{dz}{dr} = \frac{H}{c} e^{\frac{H_r}{c}} \rightarrow dr = \frac{c}{H} e^{-\frac{H_r}{c}} dz \rightarrow dr = \frac{c}{H} \frac{dz}{z + 1} \end{cases}. \quad (32)$$

Substitution into (31) then gives the final formula for comparison with experimental data

$$A = 4\pi n_{q_0} \left(\frac{c}{H}\right)^3 \rightarrow \boxed{\frac{dN}{dz} = A \frac{(\ln(z + 1))^2}{z + 1}}. \quad (33)$$

The relevant data were used from The Million Quasars (Milliquas) catalog, v7.2aa, 18 October 2021 [20], which contains experimental data obtained by observing about 977 000 sources. The fit of the theoretical dependence (33) to these experimental data is shown in Fig. 3.

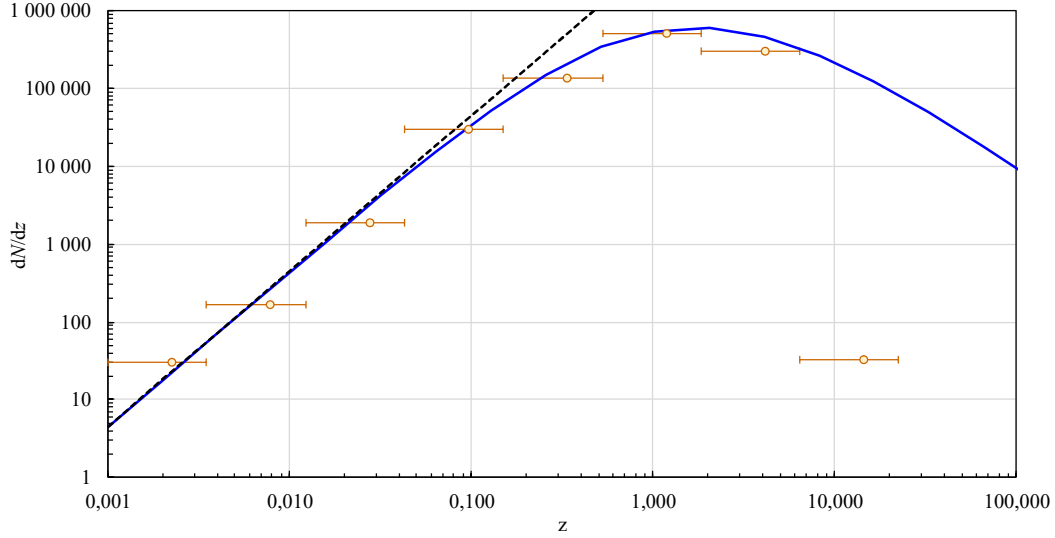


Fig.3 Theoretical fit — of the dependence of the number of quasars with the increase in redshift dN/dz on the magnitude of their redshift z (for parameter $4.5 \cdot 10^6$) [20]. Hollow points correspond to the average of all measured z values within respective interval and horizontal line define its width. The black dashed line corresponds to a uniform distribution of sources in flat space with Euclidean metric E3 and the standard linear form of Hubble's law for redshift.

The requirement of the fit is again the limit transition $z \rightarrow 0$ of equation (33) to the standard version of the Minkowski metric at small distances from the COP. This requirement of asymptotic behaviour is satisfied by the transition of the function (33) to the standard form z^2 . The theoretical shape of the fit function is confronted in good agreement with the number of quasars in the first six statistical intervals, which are shown in Fig. 3 as horizontal lines. The calculated coefficient of determination $R^2 \approx 0.9511$ for the first six points characterise a partial agreement between theory and experiment. Using the regression parameter $A \approx 4.5 \cdot 10^6$ in equation (33) we can estimate the quasar number density in the universe to $n_{q_0} \approx 1.55 \cdot 10^{-73} \text{ m}^{-3} \approx 4559 \text{ Gpc}^{-3}$.

Similarly to the previous section, we can also justify the deficit in the number of sources in the last interval for high values of z . And again, additional measurements could serve to partially verify the hypothesis of a global conformal metric of the universe.

6. OLBERS' PARADOX AND THE OBSERVABLE UNIVERSE

The assumption of a luminous sky in the visible light region (Olbers' paradox) does not match experimental experience, and in a universe with a fully conformal metric (1) this paradox can be explained via redshift. Assume that on sufficiently large cosmological scales the number density of astrophysical light sources n can be approximated by a constant. Let us introduce the intensity contribution of the average model sources dI_Ω from the differential volume dV oriented towards the COP. According to the classical Olbers' paradox, the intensity contribution of light from the differential volume dV at a distance r from the COP will be

$$dI_{\Omega}(r) = \left(\frac{d^2\varepsilon(r)}{dt(r)dS(r)} \right) ndV = \left(\frac{d^2\varepsilon(r)}{dt(r)dS(r)} \right) nd\Omega r^2 dr. \quad (34)$$

As a result of the metric transformation of the derivative variables (26), it decreases exponentially with distance r from the COP

$$\text{metric transformation} \rightarrow \left\{ \begin{array}{l} dt(r) = dt(0)e^{\frac{H}{c}r} \\ dS(r) = dS(0)e^{\frac{2H}{c}r} \end{array} \right\} \rightarrow dI_{\Omega}(r) = \left(\frac{d^2\varepsilon(r)}{dt(0)dS(0)} \right) e^{-\frac{3H}{c}r} nd\Omega r^2 dr. \quad (35)$$

For simplicity of the model derivation, assume purely thermal emission from an average model source with surface temperature $T(0)$. After including all the mentioned effects, the intensity contribution dI_{Ω} (35) takes the form

$$\begin{array}{l} \text{inverse square law} \rightarrow \frac{d^2\varepsilon(r)}{dt(0)dS(0)} = \left(\frac{\sigma T(r)^4}{\pi} \right) \frac{1}{r^2} \\ \text{redshift+Wien's law} \rightarrow \frac{T(r)}{T(0)} = \frac{\nu_{\max}(r)}{\nu_{\max}(0)} = e^{-\frac{H}{c}r} \end{array} \rightarrow \left\{ \begin{array}{l} \frac{d^2\varepsilon(r)}{dt(0)dS(0)} = \left(\frac{\sigma T(0)^4}{\pi} \right) \frac{e^{-4\frac{H}{c}r}}{r^2} \\ dI_{\Omega}(r) = \left(\frac{\sigma T(0)^4}{\pi} \right) e^{-7\frac{H}{c}r} nd\Omega dr \end{array} \right. \quad (36)$$

The experimentally measured intensity $I_{\Omega}(R)$ [$\text{Wm}^{-2}\text{sr}^{-1}$] in the direction of the unit angle axis is the sum of all contributions from the opposite half-space 2π to the distance R of the observation horizon

$$I_{\Omega}(R) = \iiint_{V_R^{2\pi}} dI_{\Omega} = \int_0^R \int_0^{2\pi} \left(\frac{\sigma T(0)^4}{\pi} \right) e^{-7\frac{H}{c}r} nd\Omega dr = 2\pi \left(\frac{\sigma T(0)^4}{\pi} \right) n \int_0^R e^{-7\frac{H}{c}r} dr. \quad (37)$$

Without knowledge of the model parameters n and $T(0)$, the dependence of the intensity $I_{\Omega}(R)$ on the distance R from the COP can be characterized by the function $\Phi(R)$, which is defined by the parametric integral in (37)

$$\Phi(R) = \int_0^R e^{-7\frac{H}{c}r} dr = \frac{1 - e^{-7\frac{H}{c}R}}{7\frac{H}{c}}, \quad (38)$$

and its graph is shown in Fig.4.

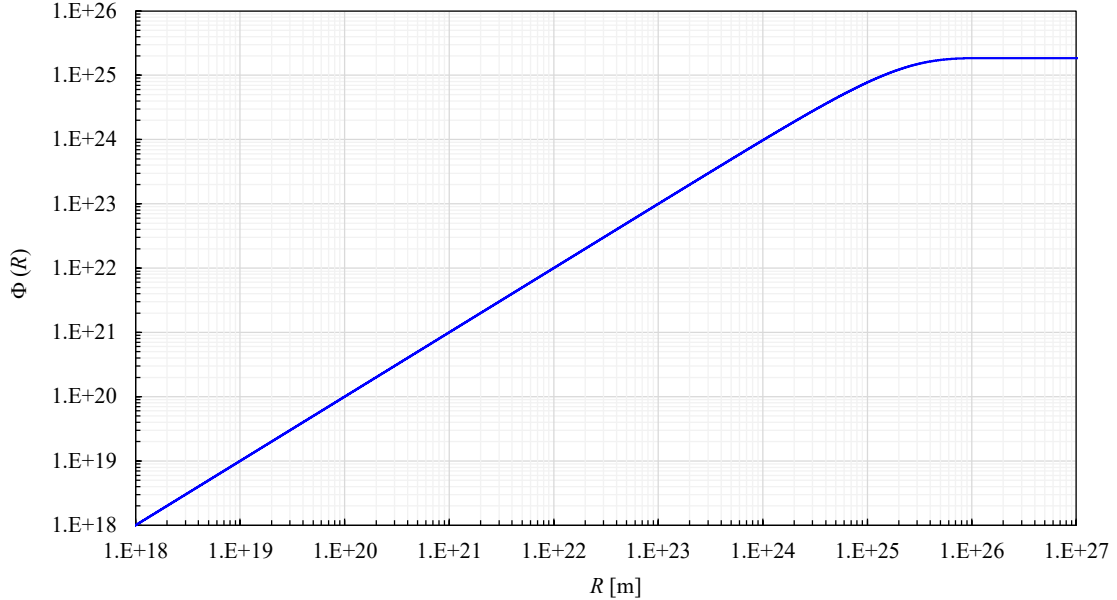


Fig.4 Dependence of the function $\Phi(R)$ (38) on the distance R of the observation horizon from the COP. The plateau of the total intensity corresponds to a slightly smaller radius than predicted $R_{obs} \approx 4.3 \cdot 10^{26}$ m by the calculations of the standard model [21].

The asymptotic behaviour of the dependence (38) leads to the final value of the total intensity $\max I_{\Omega}$

$$\max I_{\Omega}(R) = \lim_{R \rightarrow \infty} I_{\Omega}(R) = \frac{2n\sigma T(0)^4}{7 \frac{H}{c}} \ll \infty, \quad (39)$$

which is approximately reached already at distances of the order of $R \approx 10^{26}$ m, and the outer region contributes negligibly. This is how the problem of the Olbers' paradox is solved within the fully conformal metric.

While in a space with a standard Minkowski metric the radiation of all differential spheres would contribute equally to the total intensity at the COP, under the conditions of a conformal metric there is a kind of limit at which the differential contributions to the total intensity drop significantly to negligible values. This decrease can be expressed on the basis of relation (36) in the form

$$\Psi(r) = \frac{dI_{\Omega}(r)/dr}{dI_{\Omega}(0)/dr} = e^{-7 \frac{H}{c} r}. \quad (40)$$

The dependence (40) is plotted in Fig. 5. The radial distance $r = 4 \cdot 10^{26}$ m from the COP, at which the intensity contribution drops by nine orders of magnitude to 1 ppb of the original value, agrees very well with the $R_{obs} \approx 4.3 \cdot 10^{26}$ of the observable universe according to the standard model [21].

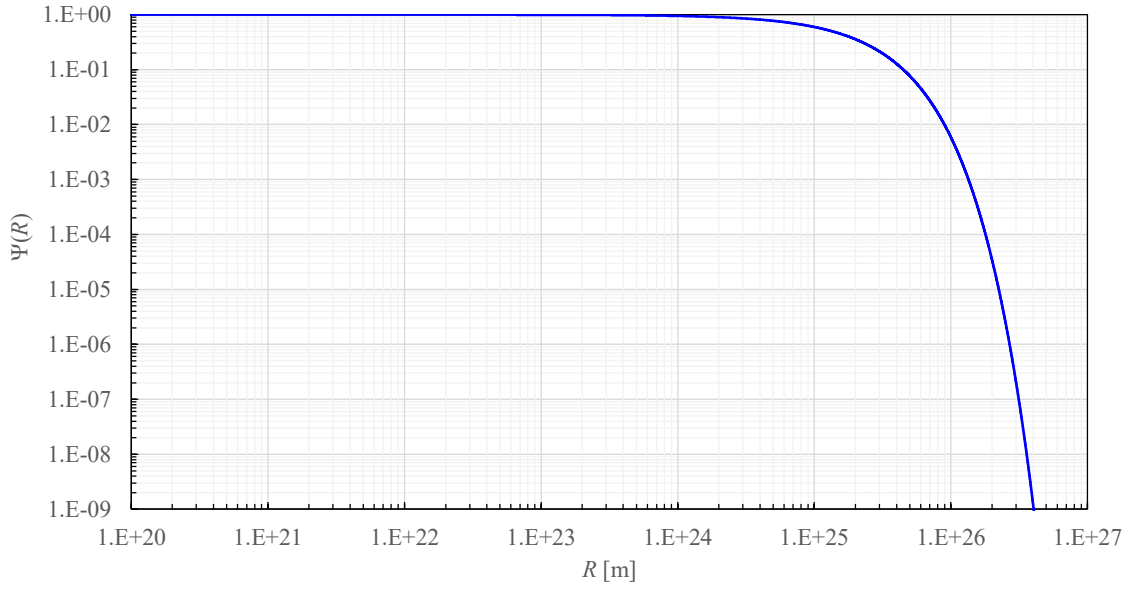


Fig.5 Dependence of the relative contributions $\Psi(R)$ (40) of the differential layer at the distance R to the total intensity at the COP.

The fully conformal metric thus defines a region of the observable universe where the contributions from the outer region are not zero in principle as in the case of the standard model, but they are completely negligible from an energy perspective. According to one of the most recent observations from the James Webb Telescope in 2022 [22], we can consider detecting objects with redshifts up to $z = 12$, which according to (22), corresponds to a distance of $3.5 \cdot 10^{26}$ m located the steep intensity drop of nine orders of magnitude in Fig. 5.

7. SEELIGER'S GRAVITATION PARADOX SOLUTION

Seeliger's gravitational paradox points out an important problem of an infinite static universe. According to standard Newtonian theory, every body is subject to the weak gravitational field of all homogeneously distributed masses in infinite 3D space. Their superposition corresponds to an infinite field strength in all directions, which is compensated by space isotropy. So Seeliger concludes that "either the universe cannot be infinite, or that Newton's law of attraction must be modified". To support the second eventuality, he proposed to add a phenomenological factor $e^{-\lambda r}$ to the gravitational force [23], [24]. At a global geodetic distance r , the scalar intensity K of the weak gravitational field of a point mass m is given by the Newtonian approximation

$$K = G \frac{m}{r^2}. \quad (41)$$

Considering that the geodesic distance r is a global parameter, we will take the intensity formulation (41) as covariant in terms of the COP position. The motion of the test unit point mass in the specified intensity field K is then generally determined by the equation of motion

$$\left[\frac{d}{dt} \left(\frac{dr}{dt} \right) = a \right] = K. \quad (42)$$

In the vicinity of the COP, the space-time has the character of the Minkowski metric and we can use the local coordinate formalism (r_o, t_o) . The equation of motion can then be written in local form with the new locally observable intensity K_o

$$\left[\frac{d}{dt_o} \left(\frac{dr_o}{dt_o} \right) = a_o \right] = K_o. \quad (43)$$

The acceleration a_o corresponds to the direct experimental experience of the observer in the local COP system. For small distances from the source, the dynamics of gravitational action then leads to the local equation of motion (43). This "local dynamics" is also the only experimental tool to describe the effect of distant gravitational sources on the test unit point mass in the COP. The equation (42) then describes the motion for general distances r from the centre of gravity. The theoretical kinematic acceleration a differs from the experimentally measurable a_o due to the transformation (23) of the differential $dx^\mu \rightarrow dx_\mu$ spacetime coordinates

$$(23) \rightarrow dx_\mu = dx_\mu^o e^{\frac{H}{c}r} \rightarrow \left\{ \begin{array}{l} dt = dt_o e^{\frac{H}{c}r} \\ dr = dr_o e^{\frac{H}{c}r} \end{array} \right\} \rightarrow a = a_o e^{-\frac{H}{c}r}. \quad (44)$$

The conformal metric (23) conserve velocity, but not the acceleration. Since the gravitational action of a distant source is testable in COP only by local experimental means, the general equation (42) must be modified into the local form using equation (44) and (43)

$$\frac{d}{dt} \left(\frac{dr}{dt} \right) = \frac{d}{dt_o} \left(\frac{dr_o}{dt_o} \right) e^{\frac{H}{c}r} = G \frac{m}{r^2} \rightarrow \frac{d}{dt_o} \left(\frac{dr_o}{dt_o} \right) = G \frac{m}{r^2} e^{-\frac{H}{c}r}. \quad (45)$$

Thus, the locally observable intensity K_o of the gravitational field of a point source of mass m is given by a modification of Newton's equation for gravitational intensity, which physically justifies Seeliger's original phenomenological proposal with the factor $e^{-\lambda r}$ [23], [24] for $\lambda = H/c$

$$K_o(r) = G \frac{m}{r^2} e^{-\frac{H}{c}r}. \quad (46)$$

The contribution of differential volume ($r^2 \sin \theta d\theta d\varphi dr$) of the homogeneously distributed mass density ρ in distance r is given by the differential

$$dK(\theta, \varphi, r) = G \frac{\rho r^2 \sin \theta d\theta d\varphi dr}{r^2} e^{-\frac{H}{c}r} = G\rho (\sin \theta d\theta) (d\varphi) \left(e^{-\frac{H}{c}r} dr \right). \quad (47)$$

The contribution of the above differential volume to the total scalar intensity to the z-axis

$$dK_z(\theta, \varphi, r) = \cos \theta \cdot dK(\theta, \varphi, r) = G\rho (\cos \theta \sin \theta d\theta) (d\varphi) \left(e^{-\frac{H}{c}r} dr \right) \quad (48)$$

then after integration over the whole half-space ($z \geq 0$) gives a finite value of the total scalar intensity K_z^∞ in the direction of the positive z-axis

$$K_z^\infty = G\rho \left[\int_0^{\frac{\pi}{2}} \cos \theta \sin \theta d\theta \right] \left[\int_0^{2\pi} d\varphi \right] \left[\int_0^\infty e^{-\frac{H}{c}r} dr \right] \rightarrow K_z^\infty = \frac{3}{8} Hc = 2.54 \cdot 10^{-10} m \cdot s^{-2} \ll \infty. \quad (49)$$

$$(21) \rightarrow \rho = \frac{3H^2}{8\pi G} = \rho_{\text{crit}}$$

In the case of a homogeneous spatial density distribution ρ , at each point in space the integral scalar intensity takes on a final magnitude of about $2.54 \cdot 10^{-10} m \cdot s^{-2}$ at each point in space, which satisfies the original Seeliger's condition for infinite 3D space. Also of interest here is the quantitative similarity of this gravitational background to the assumed magnitude of the Milgrom acceleration constant $2 \cdot 10^{-10} m \cdot s^{-2}$ [25] in the theory of modified Newtonian dynamics MOND.

CONCLUSION

In this paper, we formulated a relatively simple global solution of Einstein's gravity equations without a cosmological term, which takes the form of a fully conformal Minkowski metric with time scaling. This conformal

metric is globally scaled in all four spacetime coordinates by the same function of time $\psi(x_4)$. The speed of light c thus remains a universal constant, independent of time and position and the same applies for other local parameters (e.g., radiation spectra, etc.), like it is for the rest mass. Changes in the time flow observed over large distances are therefore similarly relative, as the relativistic mass change of moving particles. Given the universal character of the local quantum definition of the time unit $1s$, and the possibility of a natural choice of origin ($x_4 = 0$) in the local presence of any observer, the exponential form of the scaling function $\psi(x_4)$ is covariant. All observers that are at rest relative to the isotropic CMB field have their own local times flowing at the same rate. However, the nonlinearity of the scaling function $\psi(x_4)$ has real observable physical content and cannot be removed by formal time recalibration.

Furthermore, some astrophysical implications of the conformal metric are discussed. On cosmological scales, this global solution shows good agreement with experimental observations of the spatial distribution of real astrophysical sources such as γ -ray bursts and quasars. Without the need for a cosmological term in Einstein's equations, it yields a generalized form of Hubble's law that agrees very well with current astrophysical data even for very distant sources. The whole concept of the model was motivated by the consideration of whether cosmological redshifts could originate due to metric differences, similar to the case of gravitational redshifts in emission from very massive objects. The conformal metric field model quite naturally solves the problem of critical global density, the flatness of 3D space, and the Olbers' and Seeliger's paradox. At the same time, it replaces the strict causal horizon principle with a much softer formulation - the region of the practically observable universe. The paper also physically justifies the modification of Newton's law of gravity for infinite space proposed by Seeliger. The modifying exponential term $e^{-Hr/c}$ is uniquely quantified by the Hubble parameter and the speed of light.

It also seems, that it might be interesting for the cosmological community to analyse other physical properties of the above global metric. In particular, the implications of the nonlinear calibration of the global time coordinate could suggest a solution to the time arrow problem.

ACKNOWLEDGEMENT

I thank Prof. James Binney for his valuable advice in writing this thesis and especially for the open mind with which he was willing to help with the publication of such a controversial topic, and first and foremost I am very grateful to my wife Jeyinka for her great support in my work.

LITERATURE

- [1] J. D. Bekenstein, "Exact solutions of Einstein-conformal scalar equations," *Ann. Phys. (N. Y.)*, vol. 82, no. 2, 1974, doi: 10.1016/0003-4916(74)90124-9.
- [2] J. A. Lester, "Conformal Minkowski space-time - I. - Relative infinity and proper time," *Nuovo Cim. B*, vol. 72, no. 2, 1982, doi: 10.1007/BF02829408.
- [3] J. A. Lester, "Conformal Minkowski spacetime - II - A Cosmological model," *Nuovo Cim B*, pp. 139–149, 1983.
- [4] G. U. Varieschi, "A kinematical approach to conformal cosmology," *Gen. Relativ. Gravit.*, vol. 42, no. 4, 2010, doi: 10.1007/s10714-009-0890-y.
- [5] D. Behnke, D. B. Blaschke, V. N. Pervushin, and D. Proskurin, "Description of supernova data in conformal cosmology without cosmological constant," *Phys. Lett. Sect. B Nucl. Elem. Part. High-Energy Phys.*, vol. 530, no. 1–4, 2002, doi: 10.1016/S0370-2693(02)01341-2.
- [6] M. Libanov, V. Rubakov, and G. Rubtsov, "Towards conformal cosmology," *JETP Lett.*, vol. 102, no. 8, 2015, doi: 10.1134/S0021364015200072.
- [7] M. M. Kumar, "Some significant conformal metrics," *Nuovo Cim. A Ser. 10*, vol. 63, no. 2, 1969, doi: 10.1007/BF02756233.
- [8] M. Ibison, "On the conformal forms of the Robertson-Walker metric," *J. Math. Phys.*, vol. 48, no. 12, 2007, doi: 10.1063/1.2815811.
- [9] C. W. Misner, K. S. Thorne, and J. A. Wheeler, "MTW-Gravitation," in *Gravitation*, 2018.
- [10] P. J. . Peebles, *Principles of Physical Cosmology*. 2020. doi: 10.2307/j.ctvxrpxvb.
- [11] Kuchař K, *Fundamentals of general relativity*. Praha: ACADEMIA , 1968.
- [12] Weinberg S, *Gravitation and Cosmology*. John Wiley & Sons Inc. , 1972.
- [13] Weinberg S, *Cosmology*. Oxford Press , 2008.

- [14] NASA, “NASA/IPAC EXTRAGALACTIC DATABASE (2022): Date and Time of the Query: Sun Nov 12 09:25:30 2017PDT,” <https://ned.ipac.caltech.edu/>, 2022.
- [15] Planck 2013, “Planck 2013 results.: I. Overview of products and scientific results, Astronomy & Astrophysics manuscript no. Planck Mission,” <https://arxiv.org/pdf/1303.5062.pdf>, 2013.
- [16] M. Schmidt, J. C. Higdon, and G. Hueter, “Application of the V/V(max) test to gamma-ray bursts,” *Astrophys. J.*, vol. 329, 1988, doi: 10.1086/185182.
- [17] C. A. Meegan *et al.*, “Spatial distribution of γ -ray bursts observed by BATSE,” *Nature*, vol. 355, no. 6356, 1992, doi: 10.1038/355143a0.
- [18] NASA, “Gamma-Ray Astrophysics: NSSTC, BATSE4B, CMAXMIN TABLE ;,” https://gammaray.nsstc.nasa.gov/batse/grb/catalog/4b/4br_cmax_cmin.html, 1996. https://gammaray.nsstc.nasa.gov/batse/grb/catalog/4b/4br_cmax_cmin.html (accessed Feb. 23, 2023).
- [19] D. W. Sciama and M. J. Rees, “Cosmological significance of the relation between red-shift and flux density for quasars [1],” *Nature*, vol. 211, no. 5055. 1966. doi: 10.1038/2111283a0.
- [20] MILLIQUAS v7.9, “MILLIQUAS v7.9: Quasars, Redshifts and the ‘accelerating-expansion’ Universe.Data, sky fields, & some thoughts on the right Cosmological model,” <http://quasars.org/milliquas.htm> , 2021.
- [21] Halpern P and Tomasello N, “Size of the Observable Universe,” *Adv. Astrophys.*, vol. 1, no. 3, 2016.
- [22] Finkelstein S et al, “A Long Time Ago in a Galaxy Far, Far Away: A Candidate $z \sim 12$ Galaxy in Early JWST CEERS Imaging,” *Astrophys. J. Lett.*, vol. 940:L55, 2022.
- [23] H. Seeliger, “Ueber das Newton’sche Gravitationsgesetz,” *Astron. Nachrichten*, vol. 137, no. 9, 1895, doi: 10.1002/asna.18951370902.
- [24] Sarasua L, “Seeliger’s Gravitational Paradox and the Infinite Universe,” *Prog. Phys.*, vol. 14, no. 3, 2018.
- [25] M. Milgrom, “A modification of the Newtonian dynamics as a possible alternative to the hidden mass hypothesis,” *Astrophys. J.*, vol. 270, 1983, doi: 10.1086/161130.

APPENDIX 1.

M4 - space

$$\Gamma^{\mu}_{\nu\lambda} = \frac{1}{2} g^{\mu\alpha} (\partial_{\nu} g_{\alpha\lambda} + \partial_{\lambda} g_{\alpha\nu} - \partial_{\alpha} g_{\nu\lambda})$$

$$\Gamma^{\mu}_{\nu\lambda} = \frac{1}{2} g^{\mu 1} (\partial_{\nu} g_{1\lambda} + \partial_{\lambda} g_{1\nu}) + \frac{1}{2} g^{\mu 2} (\partial_{\nu} g_{2\lambda} + \partial_{\lambda} g_{2\nu}) + \frac{1}{2} g^{\mu 3} (\partial_{\nu} g_{3\lambda} + \partial_{\lambda} g_{3\nu}) + \frac{1}{2} g^{\mu 4} (\partial_{\nu} g_{4\lambda} + \partial_{\lambda} g_{4\nu} - \partial_{4} g_{\nu\lambda})$$

$$\begin{aligned} g_{11}(x_4) &= \psi(x_4) \eta_{11} = \psi(x_4) \\ g_{22}(x_4) &= \psi(x_4) \eta_{22} = \psi(x_4) \\ g_{33}(x_4) &= \psi(x_4) \eta_{33} = \psi(x_4) \\ g_{44}(x_4) &= \psi(x_4) \eta_{44} = -\psi(x_4) \end{aligned}$$

$$\begin{aligned} \Gamma^1_{\nu\lambda} &= \frac{1}{2} g^{11} (\partial_{\nu} g_{1\lambda} + \partial_{\lambda} g_{1\nu}) \rightarrow \begin{cases} \Gamma^1_{1\lambda} = \frac{1}{2} g^{11} \left\{ \frac{\partial_1 g_{1\lambda}}{0} + \partial_{\lambda} g_{11} \right\} = \frac{1}{2} g^{11} \partial_{\lambda} g_{11} \rightarrow \boxed{\Gamma^1_{14} = \frac{1}{2} g^{11} \partial_4 g_{11}} \rightarrow \Gamma^1_{14} = \frac{1}{2} \psi(x_4)^{-1} \partial_4 \psi(x_4) \\ \Gamma^1_{2\lambda} = \frac{1}{2} g^{11} \left\{ \frac{\partial_2 g_{1\lambda}}{0} + \partial_{\lambda} \frac{g_{12}}{0} \right\} = 0 \\ \Gamma^1_{3\lambda} = \frac{1}{2} g^{11} \left\{ \frac{\partial_3 g_{1\lambda}}{0} + \partial_{\lambda} \frac{g_{13}}{0} \right\} = 0 \\ \Gamma^1_{4\lambda} = \frac{1}{2} g^{11} \left\{ \partial_4 g_{1\lambda} + \partial_{\lambda} \frac{g_{14}}{0} \right\} = \frac{1}{2} g^{11} \partial_4 g_{1\lambda} \rightarrow \boxed{\Gamma^1_{41} = \frac{1}{2} g^{11} \partial_4 g_{11}} \rightarrow \Gamma^1_{41} = \frac{1}{2} \psi(x_4)^{-1} \partial_4 \psi(x_4) \end{cases} \\ \Gamma^2_{\nu\lambda} &= \frac{1}{2} g^{22} (\partial_{\nu} g_{2\lambda} + \partial_{\lambda} g_{2\nu}) \rightarrow \begin{cases} \Gamma^2_{1\lambda} = \frac{1}{2} g^{22} \left\{ \frac{\partial_1 g_{2\lambda}}{0} + \partial_{\lambda} \frac{g_{21}}{0} \right\} = 0 \\ \Gamma^2_{2\lambda} = \frac{1}{2} g^{22} \left\{ \frac{\partial_2 g_{2\lambda}}{0} + \partial_{\lambda} g_{22} \right\} = \frac{1}{2} g^{22} \partial_{\lambda} g_{22} \rightarrow \boxed{\Gamma^2_{24} = \frac{1}{2} g^{22} \partial_4 g_{22}} \rightarrow \Gamma^2_{24} = \frac{1}{2} \psi(x_4)^{-1} \partial_4 \psi(x_4) \\ \Gamma^2_{3\lambda} = \frac{1}{2} g^{22} \left\{ \frac{\partial_3 g_{2\lambda}}{0} + \partial_{\lambda} \frac{g_{23}}{0} \right\} = 0 \\ \Gamma^2_{4\lambda} = \frac{1}{2} g^{22} \left\{ \partial_4 g_{2\lambda} + \partial_{\lambda} \frac{g_{24}}{0} \right\} = \frac{1}{2} g^{22} \partial_4 g_{2\lambda} \rightarrow \boxed{\Gamma^2_{42} = \frac{1}{2} g^{22} \partial_4 g_{22}} \rightarrow \Gamma^2_{42} = \frac{1}{2} \psi(x_4)^{-1} \partial_4 \psi(x_4) \end{cases} \\ \Gamma^3_{\nu\lambda} &= \frac{1}{2} g^{33} (\partial_{\nu} g_{3\lambda} + \partial_{\lambda} g_{3\nu}) \rightarrow \begin{cases} \Gamma^3_{1\lambda} = \frac{1}{2} g^{33} \left\{ \frac{\partial_1 g_{3\lambda}}{0} + \partial_{\lambda} \frac{g_{31}}{0} \right\} = 0 \\ \Gamma^3_{2\lambda} = \frac{1}{2} g^{33} \left\{ \frac{\partial_2 g_{3\lambda}}{0} + \partial_{\lambda} \frac{g_{32}}{0} \right\} = 0 \\ \Gamma^3_{3\lambda} = \frac{1}{2} g^{33} \left\{ \frac{\partial_3 g_{3\lambda}}{0} + \partial_{\lambda} g_{33} \right\} = \frac{1}{2} g^{33} \partial_{\lambda} g_{33} \rightarrow \boxed{\Gamma^3_{34} = \frac{1}{2} g^{33} \partial_4 g_{33}} \rightarrow \Gamma^3_{34} = \frac{1}{2} \psi(x_4)^{-1} \partial_4 \psi(x_4) \\ \Gamma^3_{4\lambda} = \frac{1}{2} g^{33} \left\{ \partial_4 g_{3\lambda} + \partial_{\lambda} \frac{g_{34}}{0} \right\} = \frac{1}{2} g^{33} \partial_4 g_{3\lambda} \rightarrow \boxed{\Gamma^3_{43} = \frac{1}{2} g^{33} \partial_4 g_{33}} \rightarrow \Gamma^3_{43} = \frac{1}{2} \psi(x_4)^{-1} \partial_4 \psi(x_4) \end{cases} \\ \Gamma^4_{\nu\lambda} &= \frac{1}{2} g^{44} (\partial_{\nu} g_{4\lambda} + \partial_{\lambda} g_{4\nu} - \partial_4 g_{\nu\lambda}) \rightarrow \begin{cases} \Gamma^4_{1\lambda} = \frac{1}{2} g^{44} \left\{ \frac{\partial_1 g_{4\lambda}}{0} + \partial_{\lambda} \frac{g_{41}}{0} - \partial_4 g_{1\lambda} \right\} = -\frac{1}{2} g^{44} \partial_4 g_{1\lambda} \rightarrow \boxed{\Gamma^4_{11} = -\frac{1}{2} g^{44} \partial_4 g_{11}} \rightarrow \Gamma^4_{11} = \frac{1}{2} \psi(x_4)^{-1} \partial_4 \psi(x_4) \\ \Gamma^4_{2\lambda} = \frac{1}{2} g^{44} \left\{ \frac{\partial_2 g_{4\lambda}}{0} + \partial_{\lambda} \frac{g_{42}}{0} - \partial_4 g_{2\lambda} \right\} = -\frac{1}{2} g^{44} \partial_4 g_{2\lambda} \rightarrow \boxed{\Gamma^4_{22} = -\frac{1}{2} g^{44} \partial_4 g_{22}} \rightarrow \Gamma^4_{22} = \frac{1}{2} \psi(x_4)^{-1} \partial_4 \psi(x_4) \\ \Gamma^4_{3\lambda} = \frac{1}{2} g^{44} \left\{ \frac{\partial_3 g_{4\lambda}}{0} + \partial_{\lambda} \frac{g_{43}}{0} - \partial_4 g_{3\lambda} \right\} = -\frac{1}{2} g^{44} \partial_4 g_{3\lambda} \rightarrow \boxed{\Gamma^4_{33} = -\frac{1}{2} g^{44} \partial_4 g_{33}} \rightarrow \Gamma^4_{33} = \frac{1}{2} \psi(x_4)^{-1} \partial_4 \psi(x_4) \\ \Gamma^4_{4\lambda} = \frac{1}{2} g^{44} (\partial_4 g_{4\lambda} + \partial_{\lambda} g_{44} - \partial_4 g_{4\lambda}) \rightarrow \boxed{\Gamma^4_{44} = \frac{1}{2} g^{44} \partial_4 g_{44}} \rightarrow \Gamma^4_{44} = \frac{1}{2} \psi(x_4)^{-1} \partial_4 \psi(x_4) \end{cases} \end{aligned}$$

APPENDIX 2.

E3 - space

$$\Gamma_{\nu\lambda}^{\mu} = \frac{1}{2}g^{\mu\alpha}(\partial_{\nu}g_{\alpha\lambda} + \partial_{\lambda}g_{\alpha\nu} - \partial_{\alpha}g_{\nu\lambda})$$

$$\Gamma_{\nu\lambda}^{\mu} = \frac{1}{2}g^{\mu 1}(\partial_{\nu}g_{1\lambda} + \partial_{\lambda}g_{1\nu}) + \frac{1}{2}g^{\mu 2}(\partial_{\nu}g_{2\lambda} + \partial_{\lambda}g_{2\nu}) + \frac{1}{2}g^{\mu 3}(\partial_{\nu}g_{3\lambda} + \partial_{\lambda}g_{3\nu})$$

$$\Gamma_{\nu\lambda}^1 = \frac{1}{2}g^{11}(\partial_{\nu}g_{1\lambda} + \partial_{\lambda}g_{1\nu}) \rightarrow \begin{cases} \Gamma_{1\lambda}^1 = \frac{1}{2}g^{11} \left(\frac{\partial_1 g_{1\lambda}}{0} + \partial_{\lambda} g_{11} \right) = \frac{1}{2}g^{11} \partial_{\lambda} g_{11} = 0 \\ \Gamma_{2\lambda}^1 = \frac{1}{2}g^{11} \left(\frac{\partial_2 g_{1\lambda}}{0} + \partial_{\lambda} \frac{g_{12}}{0} \right) = 0 \\ \Gamma_{3\lambda}^1 = \frac{1}{2}g^{11} \left(\frac{\partial_3 g_{1\lambda}}{0} + \partial_{\lambda} \frac{g_{13}}{0} \right) = 0 \end{cases}$$

$$\Gamma_{\nu\lambda}^2 = \frac{1}{2}g^{22}(\partial_{\nu}g_{2\lambda} + \partial_{\lambda}g_{2\nu}) \rightarrow \begin{cases} \Gamma_{1\lambda}^2 = \frac{1}{2}g^{22} \left(\frac{\partial_1 g_{2\lambda}}{0} + \partial_{\lambda} \frac{g_{21}}{0} \right) = 0 \\ \Gamma_{2\lambda}^2 = \frac{1}{2}g^{22} \left(\frac{\partial_2 g_{2\lambda}}{0} + \partial_{\lambda} g_{22} \right) = \frac{1}{2}g^{22} \partial_{\lambda} g_{22} = 0 \\ \Gamma_{3\lambda}^2 = \frac{1}{2}g^{22} \left(\frac{\partial_3 g_{2\lambda}}{0} + \partial_{\lambda} \frac{g_{23}}{0} \right) = 0 \end{cases}$$

$$\Gamma_{\nu\lambda}^3 = \frac{1}{2}g^{33}(\partial_{\nu}g_{3\lambda} + \partial_{\lambda}g_{3\nu}) \rightarrow \begin{cases} \Gamma_{1\lambda}^3 = \frac{1}{2}g^{33} \left(\frac{\partial_1 g_{3\lambda}}{0} + \partial_{\lambda} \frac{g_{31}}{0} \right) = 0 \\ \Gamma_{2\lambda}^3 = \frac{1}{2}g^{33} \left(\frac{\partial_2 g_{3\lambda}}{0} + \partial_{\lambda} \frac{g_{32}}{0} \right) = 0 \\ \Gamma_{3\lambda}^3 = \frac{1}{2}g^{33} \left(\frac{\partial_3 g_{3\lambda}}{0} + \partial_{\lambda} g_{33} \right) = \frac{1}{2}g^{33} \partial_{\lambda} g_{33} = 0 \end{cases}$$

APPENDIX 4.

$$\begin{aligned}
R_{11} - \frac{1}{2}R\psi(x_4)\eta_{11} &= \kappa p \\
\frac{1}{2}\partial_4^2 \ln \psi(x_4) + \frac{1}{2}(\partial_4 \ln \psi(x_4))^2 - \frac{1}{2}\left(3\partial_4^2 \ln \psi(x_4) + \frac{3}{2}(\partial_4 \ln \psi(x_4))^2\right)\psi^{-1}(x_4)\psi(x_4)\eta_{11} &= \kappa p \\
\boxed{-\partial_4^2 \ln \psi(x_4) - \frac{1}{4}(\partial_4 \ln \psi(x_4))^2} &= \kappa p
\end{aligned}$$

$$\begin{aligned}
R_{44} - \frac{1}{2}R\psi(x_4)\eta_{44} &= \kappa \varepsilon \\
-\frac{3}{2}\partial_4^2 \ln \psi(x_4) - \frac{1}{2}\left(3\partial_4^2 \ln \psi(x_4) + \frac{3}{2}(\partial_4 \ln \psi(x_4))^2\right)\psi^{-1}(x_4)\psi(x_4)\eta_{44} &= \kappa \varepsilon \\
\boxed{\frac{3}{4}(\partial_4 \ln \psi(x_4))^2} &= \kappa \varepsilon
\end{aligned}$$

APPENDIX 5.

E3 - space

$$\left. \begin{aligned}
\partial_1 g_{\mu\nu}(x_4) &= 0 \\
\partial_2 g_{\mu\nu}(x_4) &= 0 \\
\partial_3 g_{\mu\nu}(x_4) &= 0
\end{aligned} \right\} \rightarrow R_{\lambda\nu} = \partial_\mu \Gamma^\mu_{\nu\lambda} - \partial_\nu \Gamma^\mu_{\mu\lambda} + \Gamma^\eta_{\nu\lambda} \Gamma^\mu_{\mu\eta} - \Gamma^\eta_{\mu\lambda} \Gamma^\mu_{\nu\eta} = 0 \rightarrow \boxed{R=0}$$

APPENDIX 6.

$$\begin{aligned}
g_{\mu\nu} &= \psi(x_4)\eta_{\mu\nu} \\
g^{\mu\nu} &= \psi^{-1}(x_4)\eta^{\mu\nu} \\
R &= R_{\mu\nu}g^{\mu\nu} = R_{\mu\nu}\eta^{\mu\nu}\psi^{-1}(x_4) = (R_{11} + R_{22} + R_{33} - R_{44})\psi^{-1}(x_4) = \left(-3\partial_4^2 \ln \psi(x_4) - \frac{3}{2}(\partial_4 \ln \psi(x_4))^2\right)\psi^{-1}(x_4) \\
R_{11} &= R_{22} = R_{33} = \frac{1}{2}\partial_4^2 \ln \psi(x_4) + \frac{1}{2}(\partial_4 \ln \psi(x_4))^2, \\
R_{44} &= -\frac{3}{2}\partial_4^2 \ln \psi(x_4) \\
R &= \left(3\partial_4^2 \ln \psi(x_4) + \frac{3}{2}(\partial_4 \ln \psi(x_4))^2\right)\psi^{-1}(x_4) \left\{ \begin{aligned} R &= \left(3\partial_4^2 \ln e^{\pm x_4 \sqrt{\frac{4}{3}\kappa\varepsilon}} + \frac{3}{2}\left(\partial_4 \ln e^{\pm x_4 \sqrt{\frac{4}{3}\kappa\varepsilon}}\right)^2\right) e^{\mp x_4 \sqrt{\frac{4}{3}\kappa\varepsilon}} \\ \psi_\pm(x_4) &= e^{\pm x_4 \sqrt{\frac{4}{3}\kappa\varepsilon}} \geq 0 \end{aligned} \right\} \boxed{R(\psi_\pm(x_4)) = 2\kappa\varepsilon e^{\mp x_4 \sqrt{\frac{4}{3}\kappa\varepsilon}} \geq 0}
\end{aligned}$$